Journal of Power Sources 243 (2013) 451–457

Contents lists available at SciVerse ScienceDirect

Journal of Power Sources

journal homepage: www.elsevier.com/locate/jpowsour

A comparison of Fuel Cell Testing protocols – A case study: Protocols used by the U.S. Department of Energy, European Union, International Electrotechnical Commission/Fuel Cell Testing and Standardization Network, and Fuel Cell Technical Team

Ira Bloom [a,*], Lee K. Walker [a], John K. Basco [a], Thomas Malkow [b], Antonio Saturnio [b], Giancarlo De Marco [b], Georgios Tsotridis [b]

[a] Argonne National Laboratory, 9700 South Cass Avenue, Argonne, IL 60439, USA
[b] European Commission, Directorate-General Joint Research Centre, Institute for Energy and Transport, Postbus 2, NL-1755 ZG Petten, The Netherlands

HIGHLIGHTS

- The aging behavior of PEM stacks was evaluated using four duty cycles.
- Testing lasted 200 h for each duty cycle.
- The change in stack performance depended on the time at full power.

ARTICLE INFO

Article history:
Received 19 April 2013
Received in revised form
4 June 2013
Accepted 5 June 2013
Available online 14 June 2013

Keywords:
Polymer-electrolyte membrane fuel cells
Fuel cell testing
Test protocols
Fuel cell durability

ABSTRACT

Argonne National Laboratory (Argonne) and the Joint Research Centre-Institute for Energy and Transport (JRC-IET) collaborated to understand the aging behavior of polymer-electrolyte membrane stacks when operated under different duty cycles. The duty cycles were that used by the U.S. Department of Energy (DST) and the US Fuel Cell Council; the New European Drive Cycle (ECE R15); that used in IEC-TS62282-7-1 (IEC) and Fuel Cell Testing and Standardization Network; and the one proposed by the US Driving Research and Innovation for Vehicle Efficiency and Energy Sustainability Fuel Cell Technical Team (FCTT).

The stacks were cycled using the duty profile in each protocol for 200 h; stack performance was measured every 100 h. Analysis of the relative changes in the average cell potentials at 180 A showed that the rate of performance decline could be ordered as IEC > ECE R15, the latter being slightly greater than or approximately equal to DST and FCTT. Comparing this ordering to the length of time at full power in the duty cycle with the degradation rates shows that they are related. Most likely, the underlying cause of performance decline can be attributed to the manner in which the product water interacts with the stack components.

1. Introduction

Polymer-electrolyte membrane (PEM) fuel cells are being developed and characterized by many organizations throughout the world for transportation applications. Thus, effective communication and understanding of the test results are becoming more important as the pace of development accelerates.

Several organizations in the United States and Europe are developing test protocols to characterize the performance and durability of PEM stacks. A review on this topic has been published [1] and shows the types of protocols used to assess the durability of cell components, cells, and stacks.

In a previous study [2], we compared the results obtained from two protocols used to measure the polarization behavior of the PEM stack; one used by the U.S. Department of Energy (DOE) and one used by Fuel Cell Testing and Standardization Network (FCTestNet) [3,4]. Briefly, the method used by DOE starts at open-circuit voltage (OCV); the current increases in 10 equally spaced steps to the maximum, rated current (I_{max}) for the stack; the current then decreases in the same number of steps to OCV. Both the current-increasing and -decreasing curves are reported. The FCTestNet protocol starts at almost any current greater than zero

* Corresponding author. Tel.: +1 630 252 4516; fax: +1 630 972 4516.
E-mail address: ira.bloom@anl.gov (I. Bloom).

0378-7753/$ – see front matter © 2013 Published by Elsevier B.V.
http://dx.doi.org/10.1016/j.jpowsour.2013.06.026

($I_{initial}$); increases to I_{max} in steps of 10% of I_{max}; decreases in steps of the same size to 10% of I_{max}; and finally increases using the same step size to $I_{initial}$. The FCTestNet protocol does not allow the stack to be at OCV, and only the current-decreasing portion of the measurement is reported. Thus, there could be differences in the level of humidification, which may impact the observed performance. Experimentally, we found no significant differences between the two methods in the previous study [2].

A crucial part of understanding the performance of a PEM stack is how the performance changes with time. Many methods to quantify the durability of the PEM stack have been proposed. The objective of this work was to compare the results obtained using four of these methods: the one used by DOE and the US Fuel Cell Council[1] (dynamic stress test [DST]) [3]; the one used in International Electrotechnical Commission (IEC)-TS62282-7-1 and FCTestNet [5,6], the New European Drive Cycle (European Commission for Europe [ECE] R15) [6,7], and the one proposed by the US Driving Research and Innovation for Vehicle Efficiency and Energy Sustainability (USDRIVE) Fuel Cell Technical Team (FCTT) (wet protocol only[2]) [8]. These test profiles are shown in Figs. 1–4. Two of protocols used in this study implicitly contain a set of assumptions on how a driver of a fuel-cell-powered car will operate the vehicle. For example, in the ECE R15 drive cycle, the set of assumptions includes the conditions found in busy European cities, such as low engine load and a maximum speed of 50 km h^{-1}. The DOE cycling protocol, however, is based on the power demands from a car driving around a typical American urban area, with higher speeds and more hill climbing. The other two protocols serve only as a means of benchmarking the performance of the stack.

Therefore, from the descriptions above, the level of electrochemical stress imposed by the protocol on the fuel cell or stack may differ. Data from Figs. 1–4 were used to calculate the important characteristics of each protocol, such as time at OCV and root-mean-square (RMS) power. Table 1 gives a summary of these characteristics. As the table indicates, the protocols have significant differences.

It was not known a priori, therefore, how the results of the tests conducted with the cycling protocols would compare with one another. Thus, to facilitate understanding and accelerate fuel cell adoption in transportation, it would be beneficial to have an experimental comparison of the effects of the electrochemical stresses imposed by the different cycling protocols.

2. Experimental

2.1. Argonne

A commercially available, 8-kW PEM fuel cell stack was tested at Argonne National Laboratory (Argonne). This stack had been used previously as part of a fuel cell system in a forklift truck. It went into service in the second quarter of 2010 and it was taken out of service in the third quarter of 2011, with a total of nearly 670 h of operating time in the fuel cell system. The stack was "harvested" from the fuel cell system and installed on a test stand in the Fuel Cell Test Facility at Argonne.

All testing used compressed, hydrocarbon-free air as oxidant and 99.999% H_2 as fuel. The stack was operated at nominally

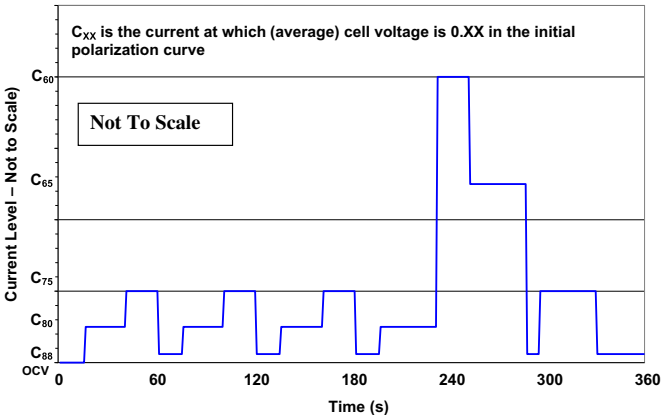

Fig. 1. Dynamic stress test (DST) duty cycle.

ambient pressure. The air and the fuel flows were regulated by mass flow controllers (MFCs). The MFCs, under computer control, opened pre-emptively to increases in demand current. Since the MFCs changed slightly before the current increased, issues associated with fuel starvation were minimized.

The stack was characterized using sequential polarization curves (a reference performance test [RPT]) in the current-increasing and–decreasing directions. The temperatures and dew points used are given in Table 2. The polarization curves were measured using constant stoichiometries of 1.2 and 2 for fuel and air, respectively. The inlet coolant flow rate and temperature were held constant. The inlet temperature was assumed to be indicative of the stack temperature. The voltage response of the stack was measured as the current was increased in 20-A steps from 0 to 200 A, and as the current was decreased likewise in 20-A steps from 200 to 0 A. A settling time of 15 min was used at each current level, except that the settling time at 0 A was shortened to 1 min. Stack power at the 200-A setting ranged from about 7 to 8.8 kW. The RPTs were performed at $t = 0$, 100, and 200 h for each profile.

The stack was cycled using the conditions shown in Table 2. The operating parameters shown reflect the manufacturer's recommendations. In some cases, these values were different from those given in the test protocol. The test profiles were applied in the sequence: DST, ECE R15, DST2, IEC, and FCTT. The total time that each profile was applied was 200 h. DST2 represents a repetition of the DST profile to check for variations. Any changes in performance were noted.

During the series of tests, the stack was idle for about 1 month for reasons unrelated to the testing. This break in testing occurred after

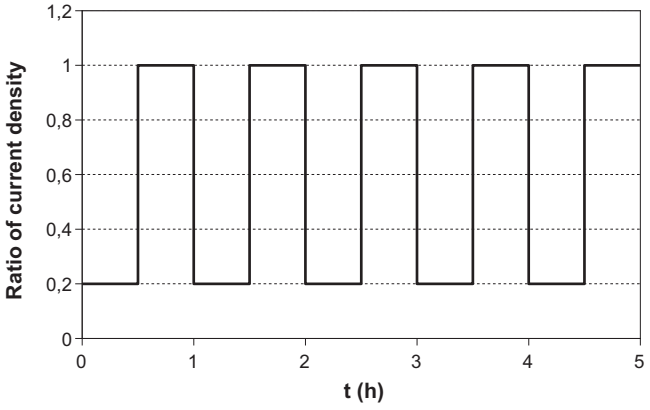

Fig. 2. Duty cycle from IEC62282-7-1 and FCTestNet.

[1] The US Fuel Cell Council is now part of the Fuel Cell and Hydrogen Energy Association (FCHEA).

[2] The FCTT "wet" protocol uses 92% relative humidity. There also is a "dry" version where the dew point is lower (25% relative humidity), and, thus, relies on self-humidification to keep the membrane hydrated. The "dry" protocol also uses a lower maximum current density, 0.1 A cm^{-2}, as compared to that used in the "wet" protocol, 1.2 A cm^{-2}.

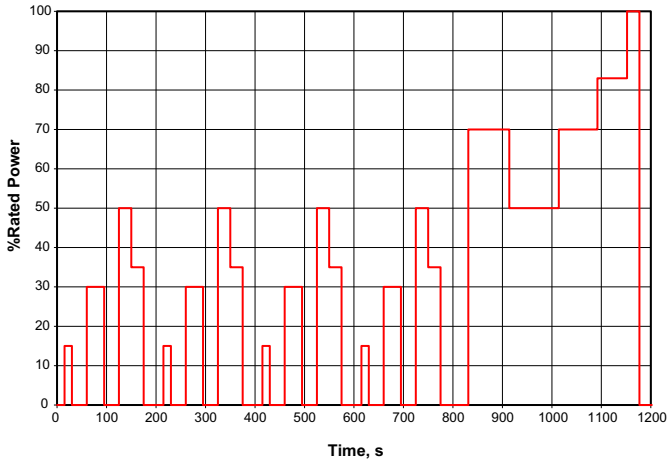

Fig. 3. New European Driving Duty Cycle (ECE R15). This profile was adapted from the original ECE R15 cycle by relating speed to power and squaring the pulses.

the second use of the DST profile. The test results are treated separately for the two time periods. The test period before the break in testing is denoted as Period 1, and that after the break, Period 2. As at the beginning of Period 1, a polarization curve was used to characterize the stack performance at the start of Period 2 and served as a reference point for the following polarization curves.

2.2. JRC-IET

A 10-kW polymer-electrolyte fuel cell (PEMFC) stack, which was designed for transportation, was tested at the Joint Research Centre-Institute for Energy and Transport (JRC-IET). This stack was used as part of a round-robin test to compare the polarization-curve results obtained by many organizations using standard test protocols and had been operated for about 900 h before being used for this experiment.

As described above for the 8-kW stack, all testing used compressed, hydrocarbon-free air as oxidant and 99.999% H_2 as fuel. The stack was operated at nominally ambient pressure. The air and the fuel flows were regulated by mass flow controllers (MFCs). The MFCs, under computer control, opened pre-emptively to increases in demand current. Since the MFCs changed slightly before the current increased, issues associated with fuel starvation were minimized.

Similar to the procedure at Argonne, the stack was characterized using sequential polarization curves (an RPT) in the current-

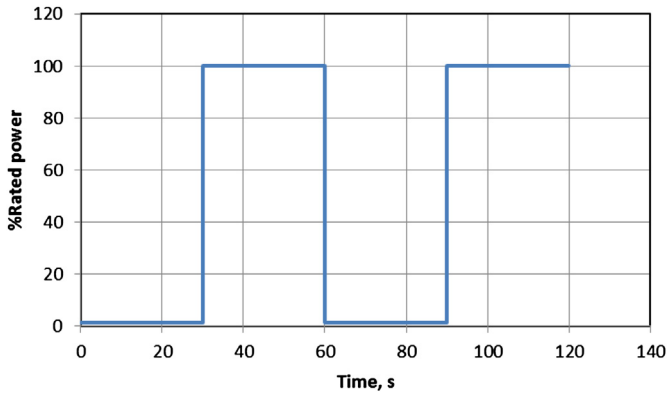

Fig. 4. FCTT duty cycle (wet).

Table 1
Characteristics of the cyclic test profiles used in this study.[a]

Profile name	Time per cycle, s	Energy, Wh cycle^{-1}	RMS power, W (cycle)	Time at OCV, s (% of cycle at OCV)	Time at full power, s
DST	360	300.1	3734.6	15 (4.2)	20
IEC	3600	5232.3	5959.0	0 (0)[b]	1800
ECE R15	1200	1154.9	4019.6	455 (37.9)	25
FCTT	60	62.2	5193.7	0 (0)[c]	30

[a] The power and energy values are from the 8-kW fuel cell stack used in this study.
[b] The minimum current specified in the IEC protocol is 20% of the maximum current.
[c] The minimum current specified in the FCTT protocol is 0.02 A cm^{-2} (~2% of the maximum current).

increasing and -decreasing directions. The temperatures and dew points used are given in Table 3. The polarization curves were measured using constant stoichiometries of 1.75 and 2.75 for fuel and air, respectively. The inlet coolant flow rate and temperature were held constant. The coolant outlet temperature was considered to be indicative of the temperature of the stack. The voltage response of the stack was measured at currents of 2, 10, 20, 40, 80, 120, 160 and 200 A, and as the current was decreased in the reverse of the steps given. A settling time of 15 min was used at each current level. Stack power at the 200-A setting ranged from about 5 to 8.8 kW. The RPTs were performed at $t = 0$, 100, and 200 h for each profile.

3. Results

3.1. Argonne

After using three sequential polarization curves to characterize the stack's operating characteristics, the profiles were used sequentially for 200 h each to "age" the stack. In general, the performance of the stack decreased with age.

Polarization curves, taken in the current-increasing and current-decreasing directions, are shown in Fig. 5. These curves were taken during the first DST aging period. As can be seen from the figure, there is minimal hysteresis between the curves, on the order of only ~12 mV. This minimal extent of hysteresis is typical of that observed throughout this work.

Typical changes in the polarization behavior of the stack are shown in Figs. 6 and 7, respectively. The figures show the changes arising from using the DST profile and those arising from the ECE

Table 2
Operating conditions for the 8-kW stack.

Test protocol	Temperature, °C	Dew point temperature, °C (cathode/anode)	Mode (constant flow or constant stoichiometry) at constant pressure[b]	Maximum utilization, % (cathode/anode)
DST	80	64/73[a]	Constant stoichiometry[c]	50.0/83.4
IEC	80	64/73	Constant flow[d]	50.0/83.4
ECE R15	80	64/73	Constant stoichiometry	50.0/83.4
FCTT	80	64/73	Constant flow	50.0/83.4

[a] These dew point temperatures correspond to relative humidity values of 50 and 74%, respectively, for the cathode and anode gases.
[b] The inlet pressure for the anode and cathode gases was 100 kPa (gauge).
[c] The stoichiometry changed with current: the fuel stoichiometry varied from 4.2 (low current) to 1.2 (high current); the air stoichiometry varied from 2.5 to 2.
[d] Gas flow was held constant. The effective utilizations at the high current levels were 83.4% and 50% for fuel and air, respectively.

Table 3
Operating conditions for the 10-kW stack.

Test protocol	Temperature, °C	Dew point temperature, °C (cathode/anode)	Mode (constant flow or constant stoichiometry) at constant pressure[b]	Maximum utilization, % (cathode/anode)
DST	65	50/58[a]	Constant stoichiometry[c]	36.3/57.1
ECE R15	65	50/58	Constant stoichiometry[d]	36.3/57.1

[a] These dew point temperatures correspond to relative humidity values of 50 and 74%, respectively, for the cathode and anode gases.
[b] The inlet pressure for the anode and cathode gases was 100 kPa (gauge).
[c] The fuel stoichiometry was 1.75; the air stoichiometry was 2.75.
[d] The fuel and air stoichiometries varied with current: the fuel stoichiometry varied from 1.75 to 3; the air stoichiometry varied from 2.75 to 4.

R15 profile. The polarization curves shown in these figures were taken in the current-increasing direction. The time interval between the successive polarization curves was approximately 100 h, with RPT0 representing the polarization curve obtained at the beginning of cycling using a particular test profile.

Changes in stack temperature, that is, the temperature difference between the coolant outlet and inlet, were also observed during each aging period. The coolant temperature rise was ~2, 2, 4, and 4 °C, respectively, for the DST, ECE R15, IEC, and FCTT tests, which are consistent with the differences in their cycle RMS power levels (Table 1).

The change in stack performance was quantified in terms of the change in average cell potential in the ohmic portion of the polarization curve. From Figs. 6 and 7, the ohmic portion of these polarization curves generally extended from ~60 to ~180 A. At lower currents, there are contributions mainly from activation polarization; at higher currents, mass-transfer losses are the dominant contributions.

With age, a decline in the stack voltage at 180 A was observed, as expected. To gauge the native performance degradation rate, the voltages at 180 A were normalized to $t = 0$ for each aging experiment. The change in average cell potential at this current was plotted in Fig. 8a for the profiles used at Argonne. From the data in Fig. 8a, the average rate of change in the relative, average cell potential is shown as a bar chart in Fig. 8b. From this figure, using the IEC profile caused the greatest apparent rate of change in relative, average cell voltage consistent with the longest duration, highest energy, greatest RMS power, and longest hold at full power per cycle (Table 1).

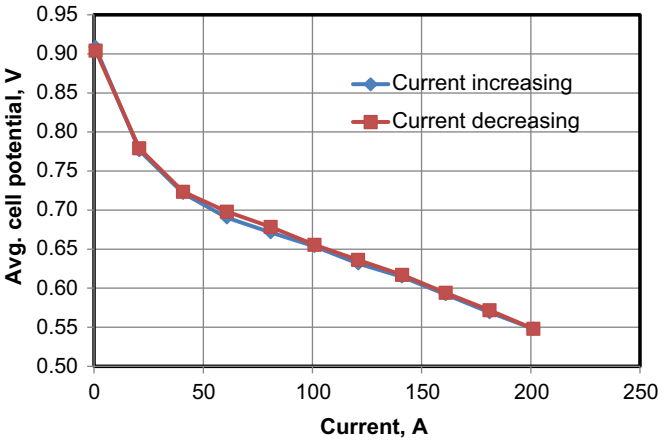

Fig. 5. Typical average cell potential vs. total current in the current-increasing and current-decreasing directions. These data are from the stack tested at Argonne and are from RPT1 during the first DST aging period. The difference between the two curves is, at most, 12 mV.

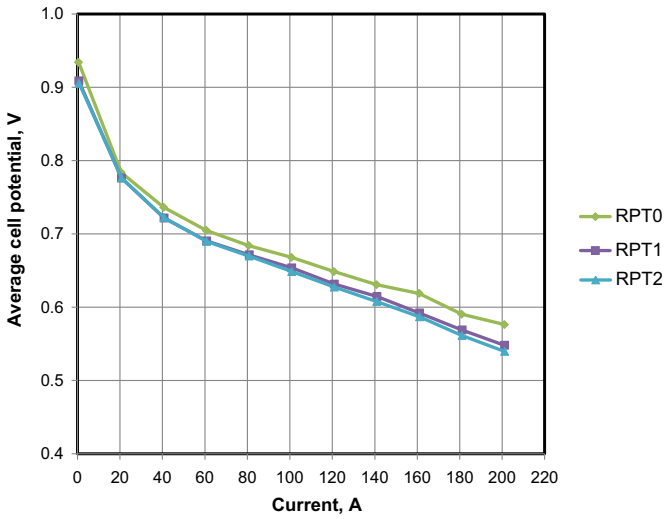

Fig. 6. Average cell potential vs. total current and time for the stack cycled using the DOE protocol at Argonne. The data in the figure represent the stack response in the current-increasing direction. The 200-A point represents the maximum current of the stack and equates to about 8.5 kW. The time between RPTs was approximately 100 h.

3.2. JRC-IET

Fig. 9a shows the typical voltage response during cycling using the DST profile. When the current rapidly increases, the stack voltage decreases quickly, possibly due to a brief increase in mass-transfer impedance. Within a short time, the stack voltage equilibrates. These observations are not seen during current-decrease transients, as expected. Similar behavior was seen using the ECE R15 profile and, at Argonne, using both profiles on the 8-kW stack.

Similar to the experience at Argonne, the performance of the stack decreased with time on testing. These changes in stack

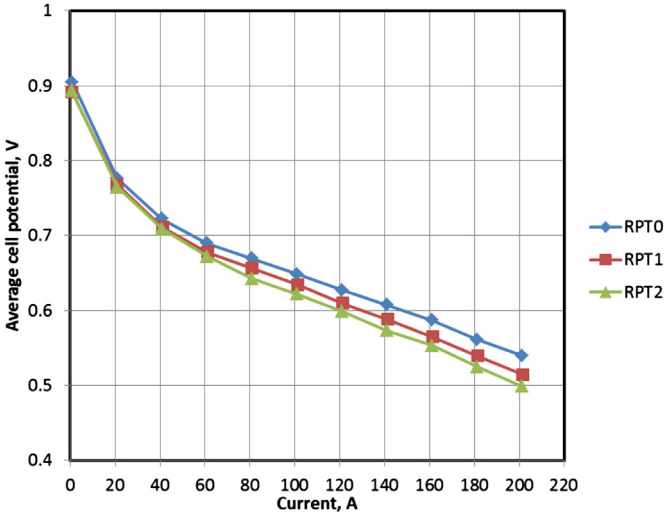

Fig. 7. Average cell potential vs. total current and time for the stack cycled using the New European Driving Cycle protocol at Argonne. The data in the figure represent the stack response in the current-increasing direction. The time between RPTs was approximately 100 h.

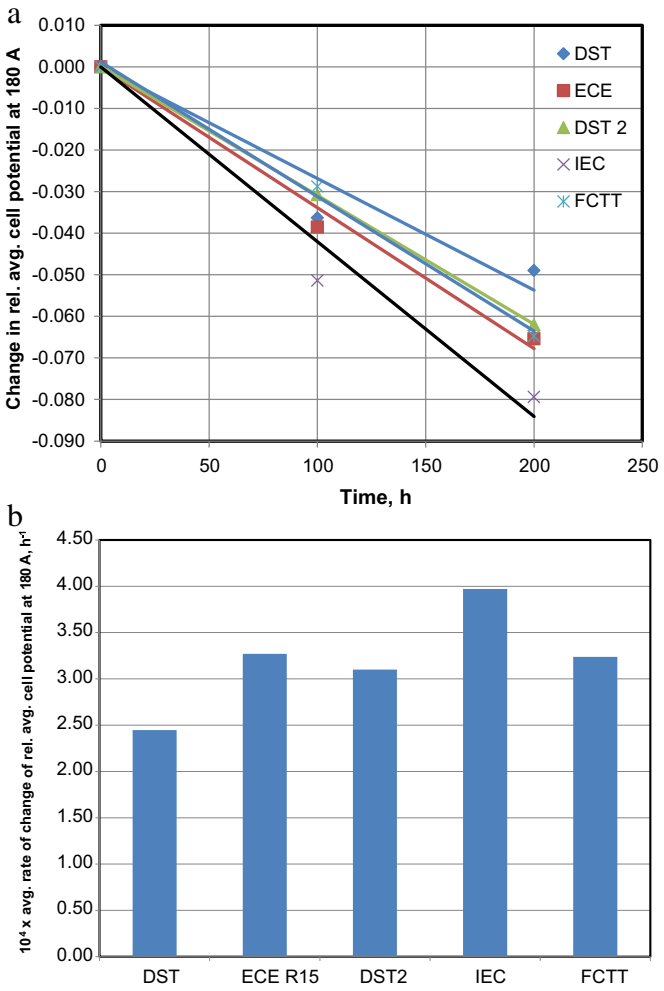

Fig. 8. (a) Change in relative, average cell potential at 180 A vs. time from the stack tested at Argonne. The lines are meant as an aid to the eye. (b) Average rate of change in relative average cell potential at 180 A vs. time for the profiles studied at Argonne. The average rate of change was calculated using the equation, Change in rel. avg. cell voltage at 200 hours/200.

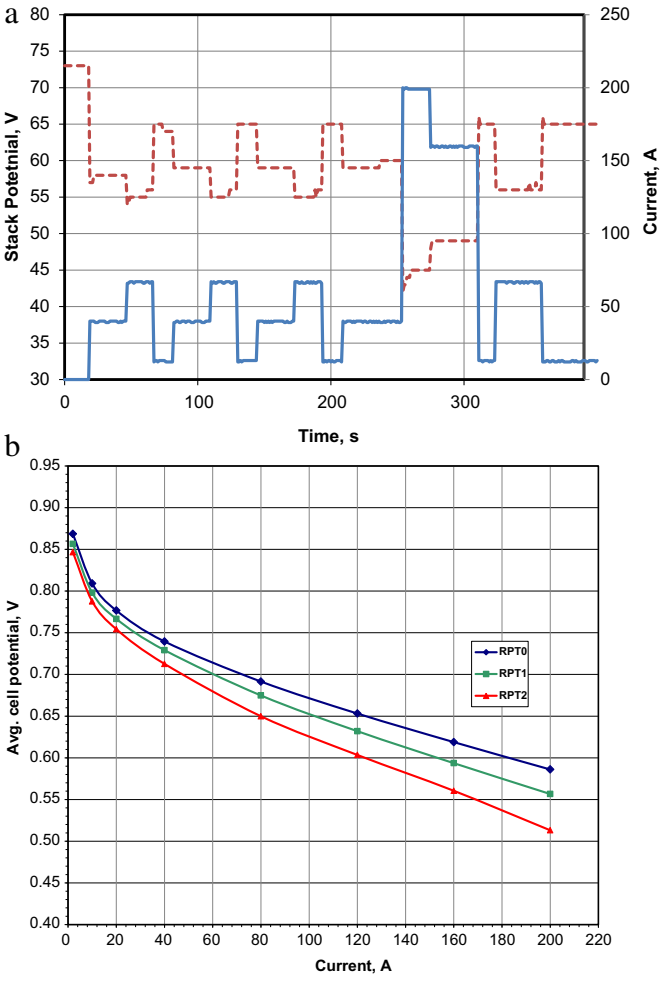

Fig. 9. (a) Stack potential and current vs. time from the stack tested at JRC-IET using the DST profile. The stack potential can be read using the scale on the left, and the current, using the scale on the right. (b) Average cell potential vs. total current and time for the stack cycled using the DOE protocol at JRC-IET. The data in the figure represent the stack response in the current-increasing direction. The time between RPTs was approximately 100 h.

performance were characterized in terms of polarization curves and are shown in Figs. 9 and 10 for those arising from the DST and ECE R15 profiles, respectively. The polarization curves shown in these figures were taken in the current-increasing direction. The time interval between the successive polarization curves was approximately 100 h, with RPT0 representing the polarization curve obtained at the beginning of cycling using a particular test profile. In both figures, the ohmic portion of the curves generally extended from ~40 to 200 A. At lower currents, there are contributions from activation polarization; at higher currents, mass-transfer losses become significant.

The changes in relative, average cell voltage for the DST and ECE R15 tests at JRC-IET are shown in Fig. 11. The average rates of change in the relative, average cell voltage were 4.7×10^{-4} h^{-1} and 5.0×10^{-4} h^{-1} for the DST and ECE R15 profiles, respectively. Within experimental error, these values are the same. Comparing these slopes to those shown in Fig. 8b shows that there was a greater difference in the degradation rates in the stack tested at JRC-IET than the one tested at Argonne, using the same profile. Most likely, the differences are due to the differences in the stacks used. It is interesting to note that, at both sites, the degradation rates caused by these profiles are very similar.

4. Discussion

The observed, high degradation rates in both stacks are likely a consequence of their histories. The stack at JRC-IET was used in a variety of tests, such as high currents, load and humidity cycling, and, possibly, fuel starvation. The stack at Argonne was used in a fork-lift truck and may have experienced similar extremes.

Usually, the performance degradation behavior of a fresh fuel cell stack is proportional to $t^{1/2}$ where time t denotes the age or test duration. Initially, there is a rapid change in performance with time. As the stack ages, the change becomes more linear with time. The fact that aged stacks were used also implies that the results would be less likely to be confounded by the rapid initial changes, making the aging results easier to interpret.

In the literature, the major sources of performance decline in PEM fuel cells are generally attributed to time at high operating potentials and unbalanced water management. At high operating potentials, greater than 0.85 V $cell^{-1}$, performance loss has been attributed to factors such as the loss of the electrochemically active area of the catalyst due to dissolution and/or particle growth [9,10].

During the normal operation of a PEM fuel cell, hydrogen and oxygen combine to make water and useful electric current. At low

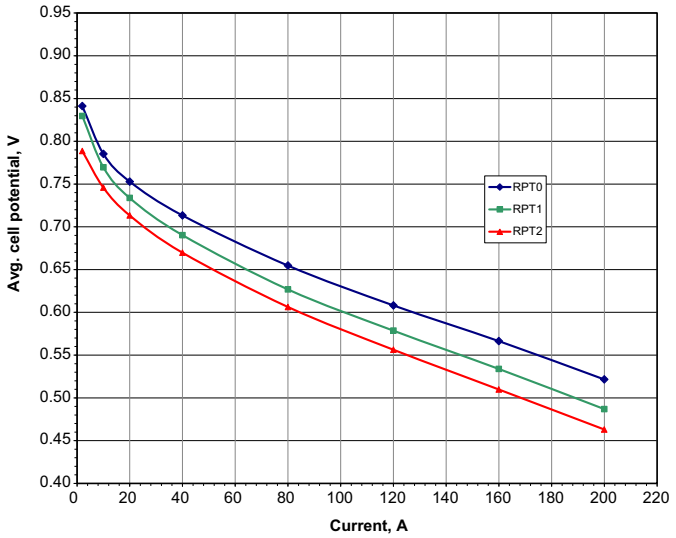

Fig. 10. Average cell potential vs. total current and time for the stack cycled using the New European Driving Cycle protocol at JRC-IET. The data in the figure represent the stack response in the current-increasing direction. The time between RPTs was approximately 100 h.

currents, small amounts of water are produced. As the current increases, more water is produced, which is both beneficial and detrimental to the performance and life of the cell and stack. The additional water (humidity) lowers the resistivity of the electrolyte membrane, thereby increasing performance. At the same time, excess water can shorten the durability of the fuel cell. Among other things, the excess water can facilitate the growth of catalyst particles through Ostwald ripening [11,12] (causes loss of the electrochemically active area); erode and dissolve the Nafion® ionomer electrolyte [12]; cause degradation of the catalyst and/or gas-diffusion layers [13]; cause flooding in the cathode gas flow channels and gas diffusion layer [14]; and leach contaminants from the cell and stack components [13–15]. Some of these effects may be reversible; others, such as leaching contaminants or loss of the electrochemically active area, obviously are not.

From the results shown above, the performance degradation rates from the duty cycles would be ordered IEC > ECE R15 slightly greater to ≈ DST ≈ FCTT. Examining the data given in Table 1 and shown in Fig. 1–4, there are three factors which could lead to differences in degradation rates: (1) RMS power, (2) time at OCV, and (3) time at maximum power (high current). In the experiments at

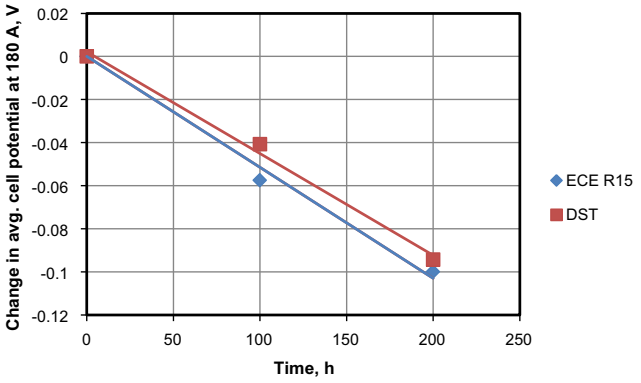

Fig. 11. Change in average cell potential at 180 A vs. time for the profiles studied at JRC-IET. The data points are indicated as markers and the least-squares fit to these data are given as solid lines.

Argonne, coolant temperature increases of ∼2, 2, 4, and 4 °C, respectively, for the DST, ECE R15, IEC, and FCTT tests were observed. If temperature rise was the source of the difference in rates, then, contrary to observation, IEC ≈ FCTT > ECE R15 ≈ DST would be the expected order. Similarly, using time at OCV as the parameter, the order would be, again, contrary to observation, ECE R15 > DST ≈ IEC ≈ FCTT.

Arranged in order of decreasing time spent at full power, the duty cycles would be IEC > FCTT > ECE R15 > DST. If the 5- and 10-s time differences at full power among the DST, ECE R15, and FCTT duty cycles produce small differences in degradation rates, then the ordering of the duty cycles by time at maximum power would closely approximate the order of the degradation rates given at the beginning of this discussion.

Even though performance degradation in PEM fuel cells can be a complex process, the majority of the loss may be attributed to one phenomenon or another. A priori, the source of the performance loss cannot be assigned to a given duty cycle characteristic. The causes of performance decline have to be determined experimentally. In the case of the study above, the loss in performance was apparently related to the time spent at full power and, thus, the amount of water produced. Exactly why this water caused the effect is beyond the scope of this study. However, it is interesting to note that the two different fuel cell stacks displayed the same behavior.

5. Conclusion

Two PEM fuel cell stacks were characterized and aged using the protocols suggested by the DOE/FCHEA, the IEC/FCTestNet, the European Union and FCTT at Argonne, and the JRCIET. The stacks were cycled using the duty profile in each protocol for 200 h, with stack performance being measured every 100 h. Analysis of the relative changes in the average cell potentials at 180 A showed that the rate of performance decline could be ordered as IEC > ECE R15, the latter being slightly greater than or approximately equal to DST and FCTT. Comparing this order to the amount of time at full power in the duty cycle with the degradation rates shows that they are related. Most likely, the underlying cause of performance decline can probably be attributed to the manner in which the product water interacts with the components of the stack.

Acknowledgments

Ira Bloom of Argonne wishes to thank his colleagues Drs. R. Kumar and D.J. Myers for many fruitful conversations. The work at Argonne was performed under the auspices of the U.S. Department of Energy, Fuel Cells Technologies Program Office, under Contract No. DE-AC02-06CH11357. The work at the JRC-IET was performed within the framework of the JRC Multi-Annual Work Program 2007–2013 under the Fuel Cell Power Chain Integration and Testing “FCPOINT” Direct Action. The research leading to these results also received funding from the Sixth Framework Programme (FP6) of the European Community on research, technological development, and demonstration activities under grant contract 020161 for the Fuel Cell Testing, Safety, and Quality Assurance (FCTesQA) Specific Targeted Research Project (STREP). It also received funding from FP5 under grant contract ENG2-CT-2002-20657 for the Research and Training Network (RTN) Fuel Cell Testing and Standardization Network (FCTESTNET).

References

[1] X.-Z. Yuan, H. Li, S. Zhang, J. Martin, H. Wang, J. Power Sources 196 (2011) 9107–9116.
[2] I. Bloom, L. Walker, J. Basco, T. Malkow, G. De Marco, G. Tsotridis, Electrochem. Soc. Trans. 30 (1) (2011) 227.

[3] Joint Hydrogen Quality Task Force, "Protocol on Fuel Cell Component Testing: Suggested Dynamic Testing Protocol (DTP), " Document USFCC 04–068 Rev A (May 1, 2006). http://www.fchea.org/core/import/PDFs/Technical%20Resources/Trans-H2Quality-DynamicTestingProfile-04-068A.pdf.
[4] FCTESTNET Test Module TM PEFC ST 5-3, Version 30 04 (2010).
[5] IEC/TS 62282-7-1, Single PEM Cell Testing Protocol (April 2010).
[6] FCTESTNET PEFC TM SC5-4 Accelerated Aging Procedure for Single Cell V. 1.2 (Oct. 2006).
[7] Wikipedia, New European Driving Cycle (12-April-2013). http://en.wikipedia.org/wiki/New_European_Driving_Cycle.
[8] US DRIVE Partnership Fuel Cell Technical Team, Cell Component Accelerated Stress Test and Polarization Curve Protocols for Polymer Electrolyte Membrane Fuel Cells (Dec. 16, 2010). www.uscar.org/commands/files_download.php?files_id=267.
[9] J.A. Gilbert, N.N. Kariuki, R. Subbaraman, A.J. Kropf, M.C. Smith, E.F. Holby, D. Morgan, D.J. Myers, J. Am. Chem. Soc. 134 (2012) 14823–14833.
[10] R.K. Ahluwahlia, S. Arisetty, Xiaoping Wang, Xiaohua Wang, R. Subbaraman, S.C. Ball, S. DeCrane, D.J. Myers, J. Electrochem. Soc. 160 (2013) F447–F455.
[11] Z. Yang, S. Ball, D. Condit, M. Gummalla, J. Electrochem. Soc. 158 (2011) B1439–B1455.
[12] J. Xie, D.L. Wood III, D.M. Wayne, T.A. Zawodzinski, P. Atanassov, R.L. Borup, J. Electrochem. Soc. 152 (2005) A104–A113.
[13] S.G. Kandlikar, M.L. Garofalo, Z. Lu, Fuel Cells 11 (2011) 814–823.
[14] S.D. Knights, K.M. Colbow, J. St-Pierre, D.P. Wilkinson, J. Power Sources 127 (2004) 127–134.
[15] T. Ha, J. Cho, K. Min, H.-S. Kim, E. Lee, J.-Y. Jyoung, Int. J. Hydrogen Energy 36 (2011) 12427–12435.